

# Sediment transport from a peatland forest after ditch network maintenance: a modelling approach

Mari Lappalainen<sup>1)\*</sup>, Harri Koivusalo<sup>2)</sup>, Tuomo Karvonen<sup>3)</sup> and Ari Laurén<sup>1)</sup>

<sup>1)</sup> Finnish Forest Research Institute, Joensuu Research Unit, P.O. Box 68, FI-80101 Joensuu, Finland  
(\*e-mail: [mari.lappalainen@metla.fi](mailto:mari.lappalainen@metla.fi))

<sup>2)</sup> Aalto University School of Science and Technology, Department of Civil and Environmental Engineering, P.O. Box 15200, FI-00076 Aalto, Finland

<sup>3)</sup> WaterHope, Munkkiniemen puistot. 20 A, FI-00330 Helsinki, Finland

Received 4 June 2009, accepted 29 Mar. 2010 (Editor in charge of this article: Eeva-Stiina Tuittila)

Lappalainen, M., Koivusalo, H., Karvonen, T. & Laurén, A. 2010: Sediment transport from a peatland forest after ditch network maintenance: a modelling approach. *Boreal Env. Res.* 15: 595–612.

The objective of this study was to describe erosion, sedimentation and transportation processes of erodible material in peatland forests after ditch network maintenance. A sediment transportation model was developed to simulate bed elevation changes in ditches and concentration of suspended solids in water. The model was suitable for simulating short-term effects (the first two years) of ditch network maintenance. The modelled spatial differences in sediment concentration were related to variation in the ditch bottom slope. The temporal variability in concentration was influenced by the water discharge rate. Other factors controlling the erosion and sedimentation in the model were the particle size of the material in bed and in suspension, the roughness height of the bed, and the Manning coefficient. Further development of the model calls for testing against comprehensive field measurements of sediment load and changes in channel dimensions.

## Introduction

Peatlands cover about one third of the land area in Finland and more than half of this area is drained for forestry purposes (Finnish Statistical Yearbook of Forestry 2005). Ditching of pristine peatlands is no longer conducted in Finland, but ditch network is maintained in order to sustain forest productivity in the drained areas. Ditch network maintenance refers to cleaning of deteriorated ditches or supplementary ditching to improve the drainage and is typically conducted every 20–40 years. The operations can cause adverse environmental effects on water-courses by increasing export of suspended solids and associated nutrients (Joensuu 2002). The

increased export mainly results from erosion of the exposed soil in the ditches (Sillanpää *et al.* 2006). Environmental effects of ditch network maintenance are typically local, the ditchings forming the main anthropogenic source of harmful load in small headwater catchments.

The contribution of ditch network maintenance to sediment loads depends on the site characteristics, the intensity of maintenance work (Joensuu 2002), and the type of peat and subsoil. Poorly decomposed peat, clay, and coarse materials tolerate erosion well (Ahti *et al.* 1995), while well decomposed peat, fine sand, and silt are more sensitive to erosion. In the areas with thin peat layer, the ditches are often cut into mineral soil (Joensuu 2002), which clearly

increases the risk of erosion. Erosion of mineral soil at the ditch bottom easily leads to a collapse of the channel banks, which further increases erosion (Joensuu 1994). Transport of suspended solids after ditch network maintenance is usually of the same or higher magnitude than transport after the initial ditching (Joensuu *et al.* 1999). The main ditches, which collect water from the upstream feeder ditches, transport the largest volumes of water and thus have a remarkable role in erosion and transportation of suspended solids.

Erosion caused by water can be divided into two processes: detachment of particles and transport of soil material. Detachment is caused by the hydrodynamic forces created by flowing water, and transport is controlled by the water flow conditions (Graf 1984). When a particle, resting on the soil surface, is no longer able to resist the hydrodynamic forces, it is first dislodged and eventually starts to move. The moving particle is deposited when the fall velocity of the particle, created by the gravity, exceeds the critical flow velocity at which the particle was detached. Flowing water in the channel with heterogeneous hydraulic conditions and soil characteristics creates different ripples and dunes, which increase the flow turbulence and complicate the soil detachment process (van Rijn 1987). Detachment is never instantaneous for a certain particle size which reflects the stochastic nature of erosion (Graf 1984). Soil material can be classified to cohesive or noncohesive according to the mechanism how it resists detachment. Noncohesive, coarse sediments resist detachment mainly by the gravity, while sediments containing a large fraction of fine-grained material, such as silt and clay, or peat, resist detachment both by the gravity and cohesion (Vanoni 2006).

In previous studies statistical-empirical approaches were applied to detect the effect of ditching and ditch network maintenance on water quality (Ahtiainen and Huttunen 1999, Joensuu 2002). The field measurements in connection with these studies were carried out manually with a weekly or monthly sampling frequency. However, since the flow conditions and the intensity of sediment transport in the ditches

can change within hours, the data of low temporal resolution do not support identification of causal relationships behind the erosion and sediment transport. Understanding the erosion process is necessary for the development of water protection methods for ditch network maintenance. A mathematical model of water flow and sediment transport processes provides an opportunity for systematic separation of the various factors controlling erosion, sedimentation, and transportation of solid material. So far only few models based on physical process description are available for describing the sediment transport in forested areas (Doten and Lettenmaier 2004, Dun *et al.* 2006), and these models focus on forest disturbance types other than ditching. The available models are mainly designed to predict sediment transport from mountainous forests where the erosion conditions greatly differ from the conditions in the topographically even peatland forests. Erosion models typically focus on the calculation of sediment yield, with less interest in local changes in the ditch network. These models were not applicable in our exercise, because the required input data were not available, the hydrological submodel was inadequate for our case, or the routines needed in calculation of local changes in ditches were lacking. The erosion models adapted for agricultural fields are not directly applicable for ditch network maintenance, because the main sediment load in the agricultural models originates from the field surface, instead of the ditches. In peatland forestry, the soil surface between the ditches is typically covered with mosses and ground vegetation, which shelter the soil from sheet erosion.

In the present study, the objective was to mathematically describe erosion, sedimentation, and transportation processes of erodible material in forest ditches after ditch network maintenance. A sediment transportation model was developed to simulate bed elevation changes in ditches and concentration of suspended solids in the water. The simulated concentrations were compared against the values measured in a main ditch of a drained forested catchment. The simulation results were used to rank the importance of the factors controlling erosion and sediment transport.

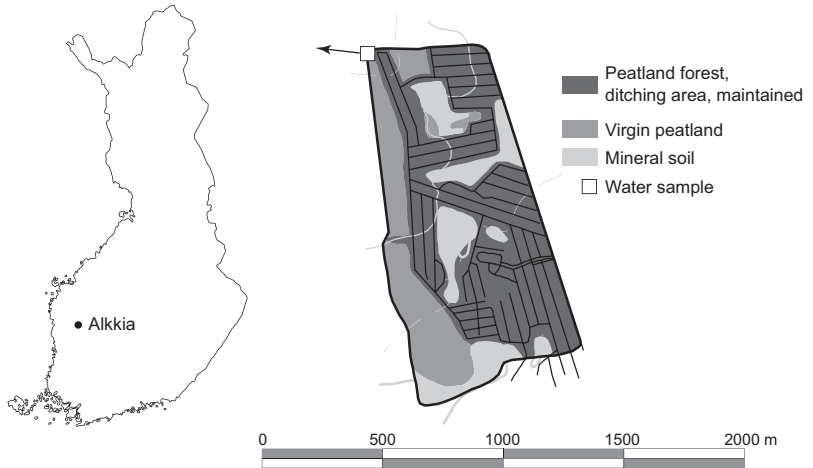


**Fig. 1.** The catchment of Alkkia.

## Material and methods

### Site description and data

Data from a catchment situated in Alkkia ( $62^{\circ}11'N$ ,  $22^{\circ}46'E$ ), Karvia, western Finland (Fig. 1) were used in the development of the model for erosion processes in the ditch network. The catchment area is 79 ha with a ditched area of about 48 ha that was drained for the first time during the 1960s. Ditch network maintenance was carried out in 1992 by cleaning the existing ditches and by constructing a sedimentation pond to reduce the load of suspended material to watercourses. According to the field measurements in 1994, the average depth and width of the main ditch were 1.3 m and 2.8 m, respectively, and the average depth and width of the feeder ditches 1.1 m and 2.5 m, respectively. The maintained ditches were dug deeper and wider than recommended by the forestry guidelines, which suggest the ditches to have a depth of 0.6–1.1 m depending on the thickness of the peat layer (Joensuu 1999). Since the peat layer thickness in the ditched area was mostly less than 0.4 m, the ditches reached the mineral soil. Mineral soil type was mostly till with a large fraction of fine particles (diameter  $< 0.06$  mm). In the southern part of the catchment mineral soil was till and sand. The dominant tree species in the area was Scots pine (*Pinus sylvestris*) with mean tree height of about 10 m in 1994.

The data used in this study were collected during the years 1992–1994 in connection with the study of forest management effects on aquatic environments (Ahti *et al.* 1995, Joensuu 2002). Water samples from the outflow in the main ditch of the drained catchment were collected at least once a week during the growing season. The concentration of suspended solids in the samples was determined by filtering the samples through a  $1 \mu\text{m}$  filter. In addition to the water sampling, the particle size distribution was measured in 1993 from the soil samples representing the material in the bottom of the main ditch and the sedimentation pond.

Daily meteorological data for the hydrological modelling were available from the Alkkia weather station ( $62^{\circ}1'N$ ,  $22^{\circ}42'E$ ) operated by the Finnish Meteorological Institute. The average annual precipitation in 1992–1994 was 709 mm (highest in 1992, 802 mm), while the average precipitation in 1971–2000 was 654 mm (Drebs *et al.* 2002, Meteorol. Yearb. Finland 1992, 1993, 1994).

### Catchment hydrological processes

The primary focus of the study was on the description of sediment processes in the main ditch of the drainage network. Since runoff from the study catchment was not continuously measured, a hydrological model was applied to pro-

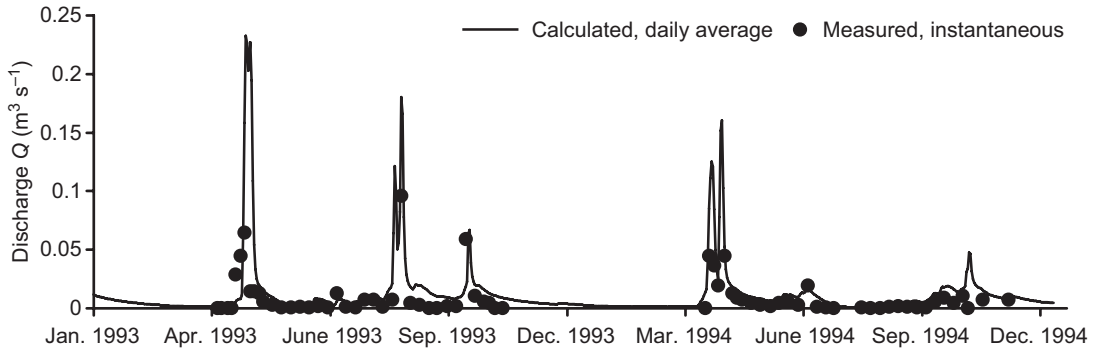


**Fig. 2.** Discharge  $Q$  ( $\text{m}^3 \text{s}^{-1}$ ) calculated by the hydrological model and measured in field.

duce the daily time series of discharge at the outlet of the main ditch. Once the outlet discharge was simulated the water level and the discharge along the main ditch were derived using the hydraulic model developed in this study. The details of the hydrological model are briefly summarised and the presentation focuses on the computation of the hydraulic and sediment transport processes.

The daily discharge from the catchment for the modelling period 1993–1994 was produced using the FEMMA model (Laurén *et al.* 2005, Koivusalo *et al.* 2006, 2008). The catchment was modelled as one-dimensional vertical column that is overlain by a tree stand and resides between two parallel drainage ditches. The model accounts for the evapotranspiration of overstorey and understorey vegetation layers, snow accumulation and melt, and vertical soil moisture distribution using soil, vegetation, and meteorological data as the inputs. The drainage flow from the soil column into the ditch was computed according to the Hooghoudt's drainage equation (e.g., El-Sadek *et al.* 2001). The water level in the ditch was set equal to the elevation of the ditch bottom, and it prescribed a boundary condition for the drainage flow computation. Ditch cleaning changes the boundary condition when the ditches are dug deeper. In FEMMA, the delay of flow in the ditch network is described using a single linear reservoir. The output from the delay routine characterised the discharge at the outlet of the main ditch and it was compared with the measured catchment discharge. The model predicted higher daily discharge peaks than were observed in the instantane-

ous flow measurements (Fig. 2). Because the measured values represent instantaneous flows, measurements may not fully characterise the daily flow volumes.

### Hydraulic processes in the main ditch

In the present study, the hydraulic flow processes that are needed in the description of channel erosion and sediment transport were modelled for the main ditch. The computation exercise was restricted to an ideal situation, because the primary aim was to improve understanding of the erosion processes and identify the main controls behind the erosion. The description of the complex channel network in the study catchment to its full extent was beyond the scope of the modelling case study. The total length (1200 m) and the topography of the modelled ditch characterised the main ditch in Alkkia. The ditch was divided into 50 calculation nodes, each having a length of 24 m (Fig. 3). An idealized rectangular cross-section (with the width of 0.88 m) was assumed for the ditch. In one computation node, erosion was assumed to change evenly the bed elevation without changing the bottom width. The discharge  $Q$  ( $\text{m}^3 \text{s}^{-1}$ ) entering the main ditch was assumed to be zero at the upstream beginning of the ditch. The outgoing daily  $Q$  from the downstream end of the main ditch was produced by the FEMMA model. Water input to the main ditch between the endpoints was assumed to occur as an inflow that is distributed evenly along the main ditch and that is equal to the outgoing daily  $Q$  (Fig. 3).

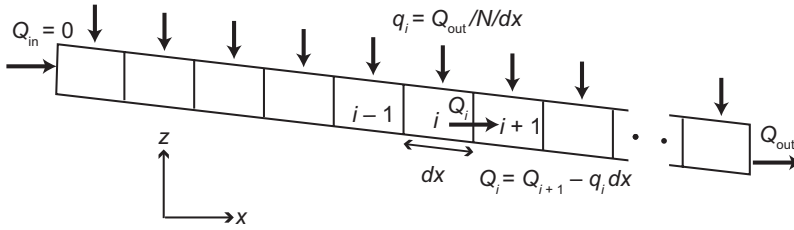


**Fig. 3.** Sketch of the one-dimensional parameterization of the main ditch. The index  $i$  refers to a ditch node, the total number of nodes is  $N = 50$ , and the length of a node is  $dx = 24$  m.  $Q_i$  is the discharge from the node  $i$  to the node  $i + 1$  and  $q_i$  ( $\text{m}^2 \text{s}^{-1}$ ) is the lateral inflow into the ditch node  $i$ .

The water depth and the flow velocity along the ditch needed to be derived before erosion could be modelled. The water depth in unsteady flow was solved using the Saint Venant equations for continuity and momentum:

$$\begin{aligned}
 b \frac{\partial h}{\partial t} + \frac{\partial Q}{\partial x} - q &= 0 \\
 \frac{\partial Q}{\partial t} + \frac{\alpha_v \partial(Q^2/A)}{\partial x} + gA \frac{\partial y}{\partial x} - gA(S_0 - S_f) &= 0
 \end{aligned}
 \tag{1}$$

where  $t$  is the time (s),  $x$  is the distance (m),  $b$  is the ditch width (m),  $h$  is the water depth (m),  $Q$  is the discharge ( $\text{m}^3 \text{s}^{-1}$ ),  $q$  is the lateral influx ( $\text{m}^2 \text{s}^{-1}$ ),  $A$  is the cross-sectional area ( $\text{m}^2$ ),  $\alpha_v$  is the velocity distribution coefficient,  $y$  is the elevation of the water surface (m),  $S_0$  is the bottom slope, and  $S_f$  is the friction slope. The Saint Venant equations were solved using the approximation of the diffusion analogy, which ignores the acceleration terms, i.e., the first two terms in the momentum equation. The momentum equation was solved in terms of  $S_f$ , which was inserted into the Manning equation:

$$\begin{aligned}
 S_f &= S_0 - \frac{\partial h}{\partial x} \\
 Q &= \frac{1}{n} AR^{2/3} \sqrt{S_f}
 \end{aligned}
 \tag{2}$$

where  $n$  is the Manning coefficient,  $R$  is the hydraulic radius (m), and  $P$  is the wetted perimeter (m). In the solution of Eq. 1, the outflow from the main ditch at each computation time step was assumed to be equal to the inflow to the ditch, and a steady-state assumption ( $dh/dt = 0$ ) was used. The following equation was solved numerically in each node and computation time step:

$$\frac{Q'_{i,j+1} - Q'_{i-1,j}}{\Delta x} - q'_i = 0; \quad i = 2, \dots, N \tag{3}$$

where  $i$  is the node index ( $N$  is the number of nodes),  $t$  is the time index, and

$$\begin{aligned}
 Q'_{i-1,j} &= \frac{1}{n} A_{i-1,j} (R_{i-1,j})^{2/3} \sqrt{\frac{y_{i-1} - y_j}{\Delta x}} \\
 Q'_{i,j+1} &= \frac{1}{n} A_{i,j+1} (R_{i,j+1})^{2/3} \sqrt{\frac{y_i - y_{j+1}}{\Delta x}} \\
 A_{i-1,j} &= 0.5(A_{i-1} + A_i) \\
 R_{i-1,j} &= 0.5(R_{i-1} + R_i) \\
 A_{i,j+1} &= 0.5(A_i + A_{i+1}) \\
 R_{i,j+1} &= 0.5(R_i + R_{i+1})
 \end{aligned}
 \tag{4}$$

where  $y_j$  is the elevation of water surface at node  $i$  (m). An applied Newton-Raphson procedure was used to find an iterative solution of the water depth in the upstream direction. The downstream end boundary condition was the known discharge  $Q_{N+1} = Q_N$ , where  $Q_N$  was produced by the FEMMA model, and the upstream end boundary condition was  $Q_{in} = 0$ . Flow velocity was derived from the discharge and the cross-sectional area of the flow.

### Sediment load

#### Model structure

The sediment transport model included computation routines for describing erosion, transportation, and sedimentation of erodible material. The model simulates bed elevation changes in a ditch, and concentration of suspended solids in flowing water. A deterministic approach was

applied to simulate detachment of particles. Particles were assumed to move when the critical threshold value of the shear stress was exceeded. The sediment load was simulated for every computation node following the method outlined for noncohesive soils by van Rijn (1987). The model accounts for the feedback from the changing bottom elevation to the channel bed slope and further on to the flow conditions. An hourly computation time step was applied in the simulation.

Sediment on the ditch bottom was described with a representative size  $d_{50}$ , corresponding to the median particle diameter. Although more complete description of sediment transport could be achieved by using several representative grain size classes (Goodell 2002), Kleinhans and van Rijn (2002) state that the use of the single-fraction approach based on  $d_{50}$  gives approximately equal results with the multi-fraction approach, when the interest is in the total transport rate.

In the model, the total sediment load was calculated as a sum of the bed load and the suspended load. The transported load in the bed load layer and the suspended load layer was assumed to be in equilibrium, which refers to an exchange of sediment between the layers to equilibrate transport, i.e., an increase in the load causes increased settling. The load equations were derived to predict the maximum load that a stream can carry in equilibrium at the given hydraulic and sedimentary condition (Graf 1984).

### Bed load

The bed load was evaluated using the approach of van Rijn (1987), which is applicable for noncohesive soils with particle sizes ranging from 0.2 to 2 mm. The thickness of the bed load layer was estimated on the basis of the bed roughness  $K_s$ , which ranges from  $d_{50}$  to  $100d_{50}$  (Liu 2001).

The bed load transport  $s_b$  ( $\text{m}^3 \text{s}^{-1} \text{m}^{-1}$ , cubic meter per second per meter of channel width) was defined as (Einstein 1950, van Rijn 1987, Liu 2001):

$$s_b = u_b \delta_b c_b \quad (5)$$

where  $u_b$  ( $\text{m s}^{-1}$ ) is the particle velocity,  $\delta_b$  (m)

is the saltation height, and  $c_b$  ( $\text{m}^3 \text{m}^{-3}$ ) is the bed load concentration. Variables  $u_b$ ,  $\delta_b$  and  $c_b$  were derived using a numerical solution of the equation of motion for a saltating particle and the analysis of experimental data (Eqs. A1–A6 in Appendix; van Rijn 1984a). The saltation layer was defined to be a layer above the bed with a thickness of about 2–10 particle diameters (van Rijn 1984a).

Van Rijn (1987) used Shields' (1936) definition for the critical shear stress as the threshold for the initial movement of particles. Following their formulation, the critical shear stress was expressed in terms of the critical Shields parameter ( $\theta_{cr}$ ) as follows:

$$\theta_{cr} = \frac{u_{*cr}^2}{(s-1)gd} \quad (6)$$

where  $u_{*cr}$  is the critical bed-shear velocity ( $\text{m s}^{-1}$ ) according to Shields (1936),  $s$  is the relative density (see Eq. A2),  $g$  is the acceleration due to gravity ( $\text{m s}^{-2}$ ) and  $d$  is the particle diameter (m). Van Rijn (1987) related  $\theta_{cr}$  to the dimensionless particle parameter  $D_*$ :

$$\theta_{cr} = \begin{cases} 0.24(D_*)^{-1} & D_* \leq 4 \\ 0.14(D_*)^{-0.64} & 4 < D_* \leq 10 \\ 0.04(D_*)^{-0.1} & 10 < D_* \leq 20 \\ 0.013(D_*)^{-0.29} & 20 < D_* \leq 150 \\ 0.055 & D_* > 150 \end{cases} \quad (7)$$

$$D_* = d_{50} \left[ \frac{(s-1)g}{\nu^2} \right]^{\frac{1}{3}} \quad (8)$$

where  $\nu$  is the kinematic viscosity coefficient ( $10^{-6} \text{m}^2 \text{s}^{-1}$ ).

### Suspended load

When the value of the bed shear velocity exceeds the fall velocity of the particles, the particles can be lifted to a level at which the upward turbulent forces are comparable to or higher than the submerged weight of the particles (van Rijn 1987). As a result the particles move into suspension. The suspended load transport  $s_s$  ( $\text{m}^3 \text{s}^{-1} \text{m}^{-1}$ ), i.e., the part of the total load that is moving without



continuous contact with the bed, was defined as

$$s_s = \int_a^h u(z) c(z) dz \quad (9)$$

where  $c(z)$  is the concentration ( $\text{m}^3 \text{m}^{-3}$ ) at the vertical level  $z$  (m), and  $u(z)$  is the velocity ( $\text{m s}^{-1}$ ) at same level (van Rijn 1987, Liu 2001, Vanoni 2006). The upper limit of the suspension layer was water surface, and the lower threshold value was defined on the basis of the bed roughness height, although it is known that the transition between the transport modes of bed and suspended load is gradual (Graf 1984). The equations for the calculation of the concentration profile,  $c(z)$ , and the corresponding velocity profile,  $u(z)$ , are shown in Appendix (Eqs. A7–A14).

Since the particles in suspension are usually considerably smaller than the bed load particles, a representative suspended particle diameter  $d_{s50}$  was determined. The diameter  $d_{s50}$  was expressed as a function of the bed particle diameter,  $d_{s50} = p d_{s0}$ , where  $p$  is the suspended particle coefficient ( $p < 1$ ).

## Mass balance

Sedimentation and erosion on the bed, and the sediment exchange between the bed and the suspension layers were taken into account using a mass balance equation (Exner 1925, van Rijn 1987, Parker *et al.* 2000). Differential equation of mass balance described the change of ditch bottom elevation over time along the modelled ditch:

$$b(1-\varphi) \frac{\partial z}{\partial t} = - \frac{\partial (b s_t)}{\partial x} \quad (10)$$

where  $\varphi$  is the soil porosity,  $z$  is the bed level above a reference (m), and  $s_t$  is the total sediment transport ( $\text{m}^3 \text{s}^{-1} \text{m}^{-1}$ ). The left-hand side of Eq. 10 corresponds to the sum of sediment pick-up rate and the deposition rate at the bed level (van Rijn 1987). The total sediment load ( $s_t$ ) was calculated as the sum of the bed load ( $s_b$ ) and the suspended load ( $s_s$ )

$$s_t = s_b + s_s \quad (11)$$

The numerical solution of the mass balance

produced the change of the channel bed elevation. Equation 10 was solved using an implicit method, which increased the numerical stability of the solution without a need for introduction of extremely short computation time steps. The solution of the bed elevation was:

$$z_i^{t+1} = z_i^t + \frac{\Delta t}{b_i(1-\varphi)\Delta x_i} \times \left\{ \alpha \left[ (b s_t)_{i-1}^{t+1} - (b s_t)_i^{t+1} \right] + (1-\alpha) \left[ (b s_t)_i^t - (b s_t)_i^t \right] \right\} \quad (12)$$

where  $t+1$  is the index referring to the new computation time step, and  $\alpha$  is the weight coefficient with a value greater than 0.5.

The increase in the bed elevation during one computation time step was limited to the level of the water surface: when  $z^{t+1}$  became higher than the water surface level,  $z^{t+1}$  was corrected to be equal to  $z^t$ , i.e. the elevation was not allowed to change. Sedimentation/erosion in the node was set to a value of zero and the sediment load from the node was set to be equal to the load in the previous node, which assured that sediment was transferred to the next node. In addition, it was assumed that the bed elevation could not become lower than the elevation in the next node downstream, i.e. in the model it was not possible to create an upward slope in the ditch. When the calculated elevation was lower than the elevation in the next node, erosion was reset to zero and the sediment load from the previous node was transferred to the next node.

## Parameterization, calibration, and sensitivity analysis

The inputs of the erosion model were the water discharge, the initial bed slope in the ditch, the bottom width of the ditch, the length of the calculation node, and the particle size  $d_{s0}$  of the bed material. The initial bed elevation in the ditch was defined from altitude contours on the map for the area. The mean slope of the ditch was 0.006. In the model, the longitudinal slope profile of the ditch was divided into different sections of the average slope, slope ranging from 0.004 to 0.013.

During the simulation, the model uses a constant value of  $d_{s0}$  in the entire ditch. Based

on the soil samples collected in 1993 from the main ditch in Alkkia, the  $d_{50}$  value of 0.2 mm was used. Although  $d_{50}$  was constant over time in the model, it is probable that bed material became coarser at locations where flowing water washed fine particles away (e.g. Rákóczy 1987, Vanoni 2006), and finer at locations where the suspended particles were deposited. Based on the field data from Alkkia and observations of van Rijn (1984b), the suspended particle coefficient  $p$  in  $d_{s50} = pd_{50}$  was assumed to fall between 0.3 and 0.9. This range was used when calibrating  $d_{s50}$  in the present model. The bed roughness height was a function of the bed particle diameter,  $K_s = kd_{50}$ , where the value of the bed roughness coefficient  $k$  was calibrated within the range from 1 to 100.

The suspended particle coefficient  $p$ , the bed roughness coefficient  $k$ , and the Manning coefficient  $n$  were the three parameters adjusted in the model calibration. After manual calibration (trial of different values) and examination of computed sediment concentration and the bed elevation change, the Manning coefficient  $n = 0.035$ , the suspension particle size  $d_{s50} = 0.8d_{50}$ , and the bed roughness  $K_s = 10d_{50} = 2$  mm were used. The weight coefficient in the implicit solution of mass balance equation (Eq. 12) was set to a value of  $\alpha = 0.8$ . The constants used in the model are shown in Table 1.

The model was found to be unstable for calculating the sediment transport during very low flow stages, when the ditch was almost dry. It was assumed that during the driest period sediment transport is negligible. In the case of very small hydraulic radius ( $R < K_s/12$ ), the bed shear velocity was set to a low value ( $10^{-5}$  m s<sup>-1</sup>), which resulted in negligible sediment transport. The assumption was necessary to run the model

**Table 1.** The constants in the model.

Constant	Unit	Value
Relative density, $s = \rho_s/\rho$	–	2.62
Kinematic viscosity, $\nu = \mu/\rho$	m <sup>2</sup> s <sup>-1</sup>	0.000001
Von Karman's constant, $\kappa$	–	0.4
Maximum bed concentration, $c_o$	m <sup>3</sup> m <sup>-3</sup>	0.65*
Porosity of soil, $\phi$	–	0.4

\* van Rijn (1987).

without instability problems through the low flow periods.

A sensitivity analysis was conducted to detect how the sediment load  $s_t$  (Eq. 11) changes when the water discharge, the initial bed slope, the representative particle size in the bed material, the suspended particle coefficient, the bed roughness coefficient, and the Manning coefficient are perturbed. The determination of the values for these variables and parameters was found to play a major role in the model simulation. The sensitivity analysis was conducted by calculating the sediment load by changing the value of one of the analyzed variables and parameters at a time. The change was  $\pm 25\%$  from the reference value that was prescribed during the model application in Alkkia. The analysis represents a hypothetical situation in particular flow conditions in a particular place.

## Evaluation of the model

To evaluate the model performance, the measured and modelled outputs were compared numerically and graphically. The compared outputs were the suspension concentrations in the outflow of the ditch. Concentration of suspended solids in water was calculated from the depth-averaged concentration:

$$\bar{c} = \frac{1}{h} \int_a^h c(z) dz \quad (13)$$

where (m<sup>3</sup> m<sup>-3</sup>) is the depth-averaged volumetric concentration in a calculation node. Concentration is calculated by multiplying with the density of the mineral soil material (2650 kg m<sup>-3</sup>).

A numerical comparison was conducted for the concentration outputs by calculating the Nash-Sutcliffe efficiency  $R_e^2$  (Nash and Sutcliffe 1970):

$$R_e^2 = \frac{S_M - S_E}{S_M} \quad (14)$$

$$S_M = \sum_{t=1}^{n_m} (M_t - M_{\text{mean}})^2$$

$$S_E = \sum_{t=1}^{n_m} (M_t - C_t)^2$$

where  $M_t$  is the measured value at time  $t$ ,  $M_{\text{mean}}$  is the mean of measured values,  $C_t$  is the calculated



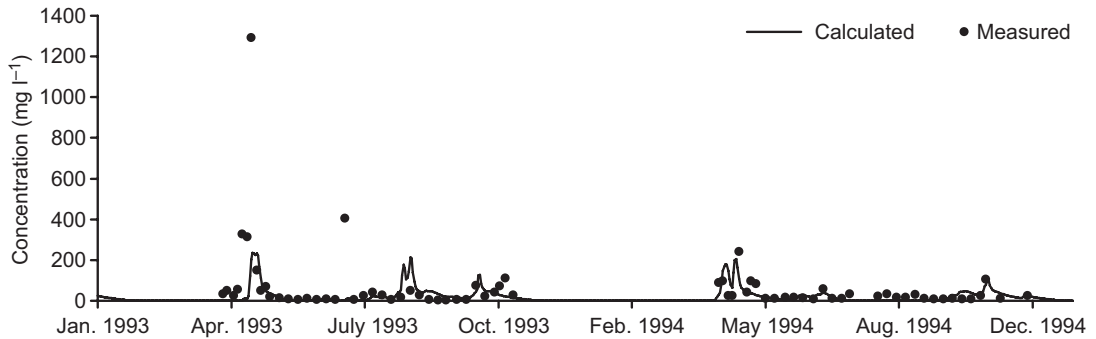


**Fig. 4.** Comparison between the measured and modelled concentrations of suspended solids in Alkkia in 1993–1994. The measured values are from the inflow to the sedimentation pond and the modeled values are from the downstream computation node 50.

value, and  $n_m$  is the number of the measurements. The model is the better the closer  $R_e^2$  is to a value of 1.

## Results

### Concentration of suspended solids

The calculated concentrations of suspended solids from the last node (node 50) at the downstream end of the ditch are compared with the measured values at the outflow of the ditch (Fig. 4). The model-produced concentrations are in the measured range, but the fit was rather poor,  $R_e^2 = 0.13$ , when all measurements from the two-year period were included in the comparison. The poor fit was explained by the observed high concentration peaks during the first year. The fit improved to  $R_e^2 = 0.43$ , when only the results from the second year were considered. The observed high concentration peaks were likely to be caused by loose soil produced during the digging. The model is not able to account for such high concentrations caused by loose soil. Joensuu *et al.* (1999) reported that the concentration of suspended solids in ditch water is not normally distributed, but small values are most common. When the highest values measured ( $> 300 \text{ mg l}^{-1}$ ) were eliminated from the concentration comparison,  $R_e^2$  was 0.30 for the calculation period of two years.

Due to the use of the equations that assume equilibrium conditions, the characteristics of a node determine the sediment concentration in the

node (Fig. 5). When the soil type was assumed to remain the same along the ditch, the main factor explaining the concentration was the bed slope. Changes in the slope were considered to have a more important role in the spatial variability of the concentration than changes in the water discharge. Discharge increased in the downstream direction in the ditch, but the highest concentration was computed for the upstream nodes, where the slope was steepest. The most influential factor controlling the temporal variability in concentration in a specific node was the water discharge. During peak flows the concentration of suspended solids was 100–1000 times higher than the lowest concentration values.

### Sediment transport and channel bed change

The total sediment transport ( $\text{m}^2 \text{ s}^{-1}$ ) was calculated in node 40 for the simulation period 1993–1994 (Fig. 6). The sediment load follows the changes in water discharge. Between the flow peaks the load is negligible. The tendency of the sediment load to follow the discharge curve is similar in all computation nodes.

Subdivision of the sediment load into the bed and the suspended loads in node 40 suggests that the main part of sediment is transported as bed load during the normal and high flows (Fig. 7). The temporal dynamics of the curves were similar in all nodes. In common, increasing water discharge increases both the bed and suspended loads. Although the bed load dominates, the frac-

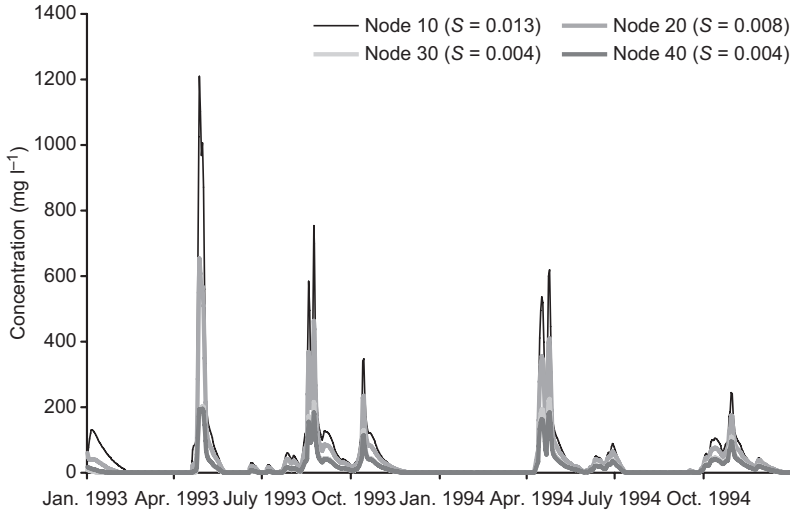


**Fig. 5.** Modelled concentration of suspended solids in nodes 10, 20, 30 and 40. S is the initial bed slope in the node.

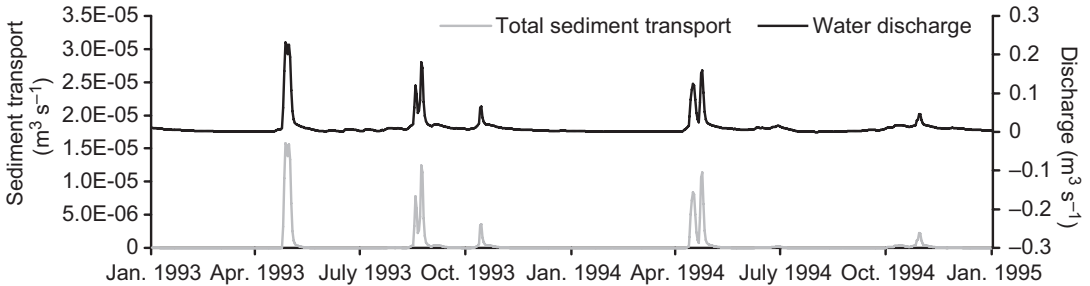


**Fig. 6.** Total sediment transport (daily average loads) and modelled daily water discharge in the Alkkia catchment in computation node 40.

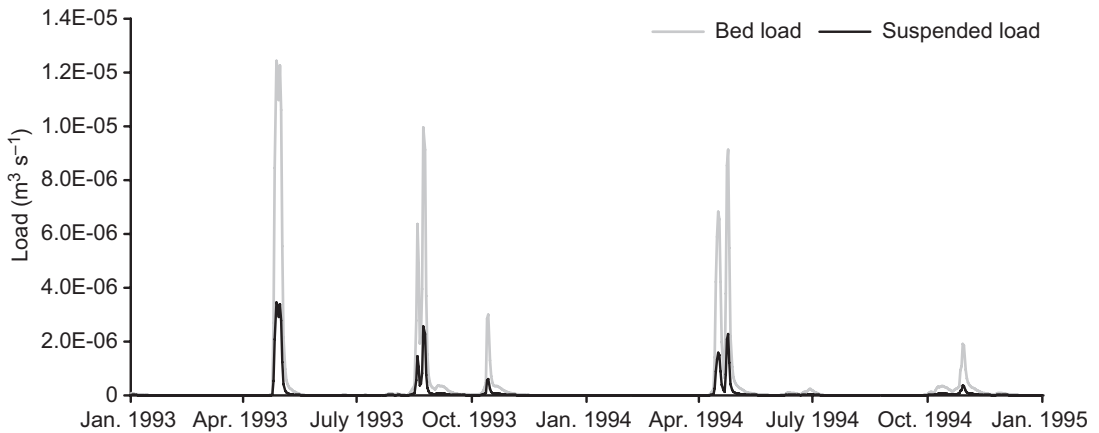


**Fig. 7.** The bed load and suspended load in node 40 during 1993–1994.

tion of the suspended load increases along with the increase of the total sediment transport.

Erosion and sedimentation changed the bed elevation in the main ditch and smoothed the slope differences along the ditch (Fig. 8). Ero-

sion was strongest in the steepest part of the ditch. The change in the bed elevation during the first year after maintenance is stronger than during the second year. The spatial changes in slope are reflected in the changes in water flow

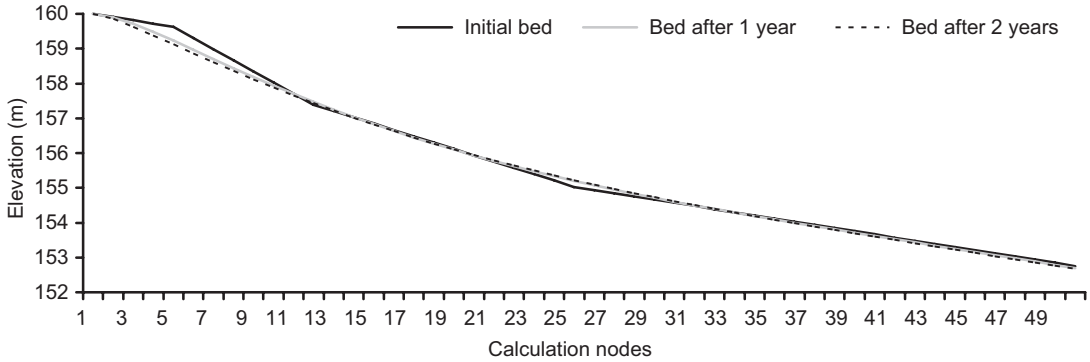


**Fig. 8.** The initial longitudinal profile and change of the bed slope in the main ditch one and two years after the ditch network maintenance in Alkkia.

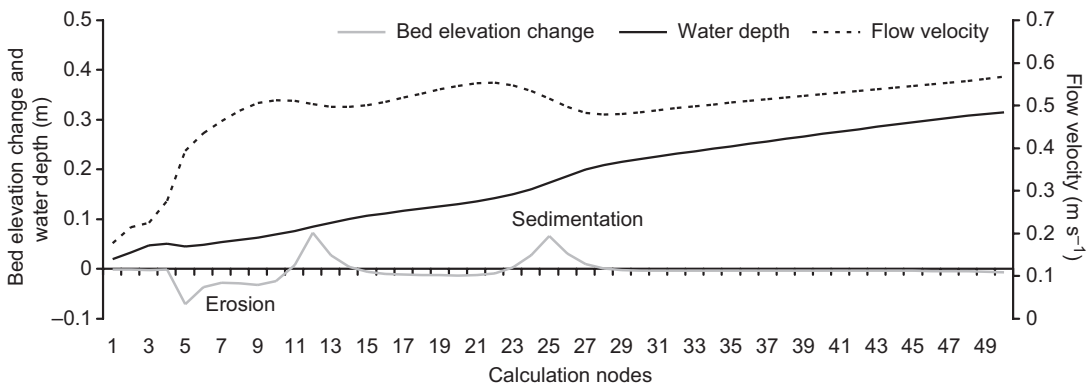


**Fig. 9.** Modelled change of the bed elevation from the initial level, and momentary depth of water and flow velocity during the spring high flow (26 April 1993).

velocity. As seen for a flood event on 26 April 1993 (Fig. 9), the flow velocity is accelerating at locations where the slope increases and decelerating where the slope decreases. From the changes in the channel bed elevation and changes in flow velocity it is possible to see that erosion and sedimentation are located in nodes where the flow velocity undergoes changes (Fig. 9).

### Sensitivity analysis

The most important factors controlling the sediment transport rate in the model were found to be the particle size  $d_{50}$  in the bed, the suspended particle parameter  $p$ , the bed roughness coefficient  $k$ , the Manning coefficient  $n$ , the discharge  $Q$ , and the bed slope  $S_0$ . The calculated sediment load was most sensitive to the perturbation in the Manning coefficient and the daily water

discharge (Fig. 10). The sediment load increases when the Manning coefficient decreases and when the water discharge increases. The effect of the Manning coefficient on the load is the stronger the smaller is the coefficient.

Even though the sediment load was found to be sensitive to the discharge rate, erosion is not only controlled by the discharge rate but also by the water flow velocity (Fig. 9). Changes in the flow velocity are mainly determined by the changes in the bed slope: increasing slope increases the load (Fig. 10). Variables other than the discharge, the Manning coefficient, and the slope in the sensitivity analysis had less influence on the load in the perturbation range of  $\pm 25\%$ .

The effect of the particle size on erosion is different for the bed load and the suspended load (Fig. 11). When the particle size increases, the bed load increases, but the suspended load decreases (Fig. 12). The relation between the

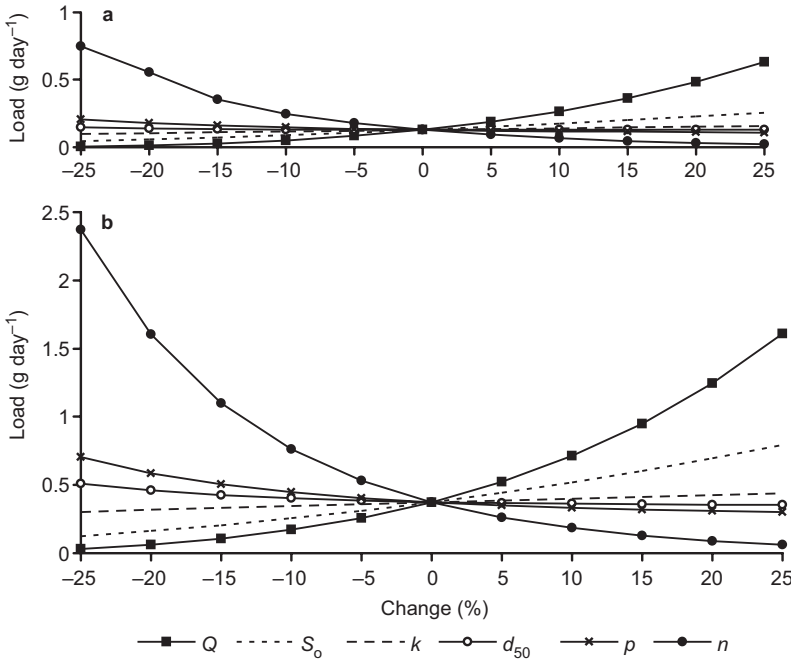


**Fig. 10.** The effect of the perturbation in the water discharge ( $Q$ ), the initial bed slope ( $S_0$ ), the representative particle size ( $d_{50}$ ), the suspended particle parameter ( $p$ ), the bed roughness coefficient ( $k$ ), and the Manning coefficient ( $n$ ) on the total sediment load, when (a)  $Q = 0.04 \text{ m}^3 \text{ s}^{-1}$ , and (b)  $Q = 0.2 \text{ m}^3 \text{ s}^{-1}$ . Reference values for the changing variables are  $S_0 = 0.004$ ,  $d_{50} = 0.2 \text{ mm}$ ,  $p = 0.8$ ,  $k = 10$ , and  $n = 0.035$ .

sediment load and the particle size is non-linear. In the case of the bed load, the load is highest for fine sand with the diameter  $d_{50}$  ranging from 0.3 to 0.4 mm. In the case of the suspended load, the load is the higher the smaller the particle size is, and the suspended load rapidly decreases when the particle size increases. When the bed material is non-uniform, the suspension particle size  $d_{s50}$  is usually smaller than  $d_{50}$  in the bed. The smaller the representative suspension particle size is in relation to the bed material, the higher the suspended load is. When the suspended load is calculated using a representative value for the particle size (percentage of the bed particle size), the correct determination of the representative particle size is important for the reliable evaluation of the total load.

## Discussion

The methods available for computing sediment transport are still incomplete. In the present study, a deterministic approach for simulating erosion was applied by assuming the particles to be detached when a critical threshold value of the shear stress was exceeded. There is criticism

against using a more or less artificial threshold value for the critical conditions (e.g. Bohling 2005) because of the stochastic nature of erosion, but in the absence of detailed field measurements the use of the threshold is the only satisfactory way to quantify erosion. The load equations are derived to predict the maximum load that a stream can carry in equilibrium at a given hydraulic and sedimentary condition (Graf 1984). When water discharge in the stream increases, there usually is an increase in the sediment transport (Graf 1984). However, the transport capacity, which refers to the maximum load that a stream can carry, is not necessarily equal to the actual load when the channel undergoes aggradation or degradation. The actual load depends on different hydrological and geological factors (Graf 1984). One flood event can remove most of the erodible material from the bed, and after the flood the stream transports considerably less material than it could carry.

The values of the calibrated parameters produced reasonable results for the calculated suspension concentration and the bed elevation change, and the values were in accordance with earlier studies (Hosia 1980, van Rijn 1987, Liu 2001). However, the representative particle size

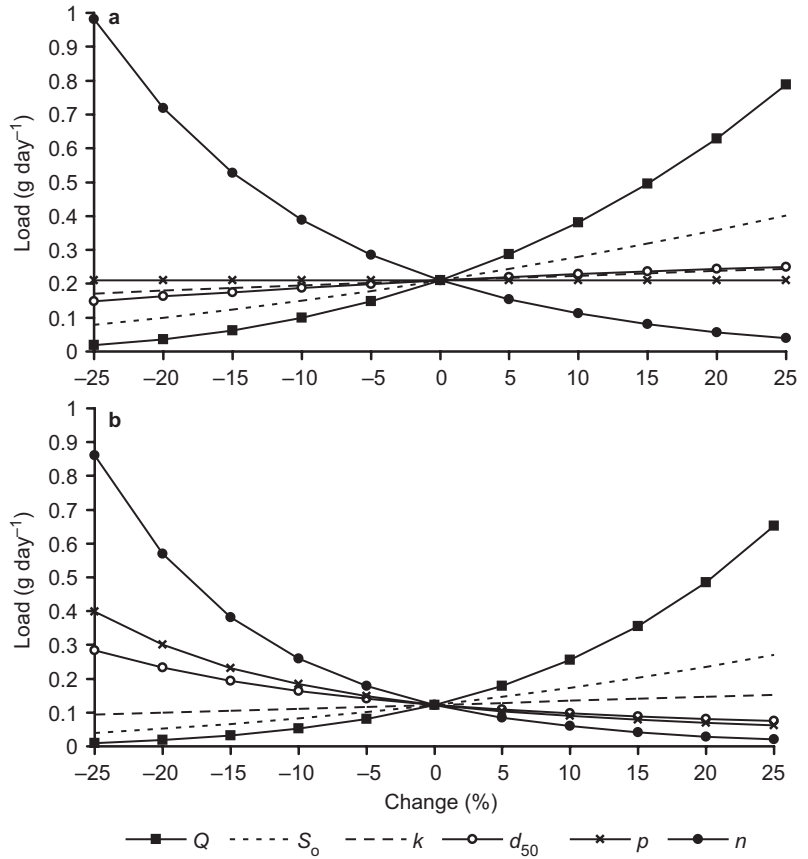


**Fig. 11.** The effect of perturbation in the water discharge ( $Q$ ), the initial bed slope ( $S_0$ ), the representative particle size ( $d_{50}$ ), the suspended particle parameter ( $p$ ), the bed roughness coefficient ( $k$ ), and the Manning coefficient ( $n$ ) on (a) bed load, and (b) suspended load. Reference values for the changing variables are  $Q = 0.1 \text{ m}^3 \text{ s}^{-1}$ ,  $S_0 = 0.004$ ,  $d_{50} = 0.2 \text{ mm}$ ,  $p = 0.8$ ,  $k = 10$ , and  $n = 0.035$ .

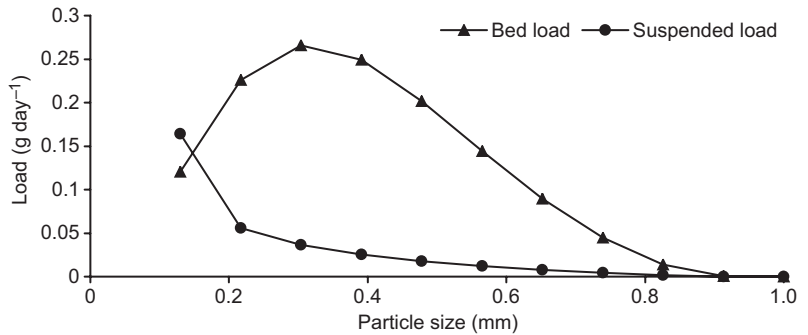


**Fig. 12.** The effect of the particle size on the sediment load ( $Q = 0.1 \text{ m}^3 \text{ s}^{-1}$ ,  $S_0 = 0.004$ ,  $k = 10$ , and  $n = 0.035$ ).

in suspension ( $d_{50}$ ) can actually be smaller than the value of  $0.8d_{50}$  used in the model, because the fine particle fraction in the modelled till soil is large and the smallest particles are most easily transported in suspension. The calculated water discharge is relatively low for most of the time which means that the transport capacity remains low and the transported particles have small size. The calibrated value of the Manning coefficient was in line with the values reported by Hosia

(1980), who suggested the Manning coefficients of 0.04 for till, 0.036 for clayey till, and 0.024 for silt. The age of the channel since digging, meanders, and vegetation in the channel affect the value of  $n$  (Hosia 1980). According to the sensitivity analysis, the effect of the Manning coefficient on the sediment load is the stronger the smaller is the Manning coefficient, which suggests that the lower the Manning coefficient is, the more carefully it needs to be determined.

The roughness height of a non-vegetated bed is reported to vary from  $2d_{50}$  to  $100d_{50}$  depending on the presence of the bed forms (van Rijn 1987, Liu 2001). In the model, the value of the bed roughness after the calibration was rather low ( $10d_{50} = 2$  mm). It can partly be explained by the ditch condition in Alkkia. The roughness height depends on the soil type, the morphology of the channel, and the determination method of the roughness height. Hosia (1980) reported the roughness height for silt to vary between 1–65 mm and for clayey till between 20–400 mm depending on the determination method. In Alkkia, the water discharge was most of the time low, which can result in a low value of bed form roughness. The erosion model is applicable only to a non-vegetated channel, which is the situation only during the first years after ditch network maintenance. In a vegetated channel bed, the hydraulic conditions differ from those in a bare soil bed and the hydraulic roughness of the bed is clearly higher compared with that of the smooth soil bottom (Hosia 1980). In the model, the roughness height was constant during the calculation period. On a rippled bed, the roughness height is a function of the particle size and the ripple height, which is affected by the flow conditions. Because flow conditions are not steady in a forest ditch, the roughness of bed forms should be related to the flow changes in addition to the particle size. By including the changing roughness of the bed forms into the model, the estimation of the sediment load could be made more realistic. Van Rijn (1984b) presented an equation to calculate the effective bed roughness, but his equation was not applicable to low flow conditions typical in Alkkia.

The determination of the particle size has an important role in the model, when a single representative value is used instead of several particle size classes. One representative particle size is difficult to determine in the case of till soil, where the particle size distribution is wide. Understanding of the erosion dynamics for a mixture of particle sizes is incomplete. The presence of cohesive fractions causes extra difficulties to the selection of the representative particle size. Commonly used representative particle size in the bed is the  $d_{50}$  value (e.g. Liu 2001, Kleinhans and van Rijn 2002, Wang *et al.* 2008), which was also used in

the present study. The model produces reasonable values for erosion from the bed and for concentration of the suspended solids, when proper values of the Manning coefficient, the roughness height, and the representative particle size in suspension are applied. It can be argued whether the selected values for the representative particle size in suspension and the roughness height of the bed correspond to the real values in Alkkia, because no measurements of the variables were available. The model did not account for differences in the soil type. It was assumed that eroded material was inorganic, because the ditches were mainly dug into mineral subsoil beneath the thin peat layer, and washout from peat was small compared with mineral soil (Joensuu 2002).

The reference level, which is used to define the lower boundary of the suspended load layer, was determined in the present study using the suggestion of van Rijn (1987). The reference level could be included in the calibration parameters. Calculation of the sediment transport in particle size classes, setting a dependency between the bed roughness and discharge, and inclusion of the hiding-exposure correction (e.g. Kleinhans and van Rijn 2002) would further improve the model. Hiding exposure refers to a phenomenon where the coarser particles in the mixture are more exposed to the flow, as the finer particles are hiding in the wake of coarser particles. The data used in the model consist of instantaneous concentration measurements from the outflow water of the catchment. Model calibration would benefit from frequent or continuous field measurements of sediment discharge and changing ditch dimensions. In order to evaluate the model applicability, the validation of the model with data not used in the calibration is necessary in the future model development.

An important finding in this study was that temporal variations in water discharge and sediment load are large and low flows cause minor erosion as compared with the high flow conditions. The relationship between spatial differences in flow velocity and sediment load, and the relationship between temporal differences in water discharge and sediment load, were both identified in the model. The highest rates of erosion occur in parts of the ditch where the flow velocity undergoes changes. Erosion and sedi-



ment transport is greatest during the flow peaks. For instance, the calculated sediment transport during the spring flood in 1993 in two weeks was equal to 46% of the sediment transport in 1993–1994. The roughness of the bed and the representative particle size were kept constant during the calculation period, and erosion reduced in time solely due to the levelling of the bed topography. Erosion in a real ditch network is reduced in locations where vegetation colonisation occurs and the bed material becomes coarser as fine fractions are washed out.

There are many sources of errors in the present model. The data used in the modelling were originally collected for other research purposes, which limited the testing of different formulas to calculate the sediment load. In principle, the erosion and sediment transport formulas should be used only in similar hydraulic conditions and with similar sediment material as originally used in the development of the formula, and the calculated sediment load should be checked against observed values. In addition, the random nature of erosion, the errors in the input data, and the modelling errors cause uncertainties in the model. Quantitative estimation of different errors would require comprehensive laboratory and field measurements.

Because of the complexity of the erosion processes, the model is only a simplified representation of the real system. The most significant differences between the model and the reality are the following: (1) Water discharge from the catchment to the modelled ditch is evenly distributed along the ditch, and does not account for the true distribution of the feeder ditches. Had the field ditches been included in the model, there would have been more drastic local changes in erosion and sedimentation in the main ditch. (2) The model is not able to simulate the pulse of sediment load caused by actual digging. Plenty of loose soil is easily washed out during and shortly after the digging operation (Joensuu 2002). (3) In the model, side wall erosion is not described. In reality erosion from the side walls can be more significant than the bed erosion. In Alkkia no deepening of the ditches was observed, which means that majority of the sediment discharge probably originates from the side walls. (4) In the present model, erosion

is not decreasing in time, but erosion continues constantly during the calculation period, depending on the water discharge. Erosion is only decreasing where the bed slope is becoming smoother. In reality, erosion decreases in time due to increasing vegetation and decreasing sediment supply in the ditch network (Vanoni 2006). On the other hand, sediment supply is increased by frost heave, or by desiccation of the ditch floor and walls during dry periods or by occasional collapse of the ditch walls.

The model application in the present study was one of the few exercises to simulate sediment transport processes in forest ditches and it provided new viewpoints to erosion in forest soils. By dividing the sediment load calculation into the bed and suspended fractions, it was possible to expand on the understanding of the different factors controlling erosion and sedimentation. According to the model simulations, the bed load has an important role in sediment transport in local scale, but its role cannot be distinguished by regular water sampling in the field. This calls for a development of the field measurement methods. The final goal in the model development is to construct a tool to assess the erodibility of forest soil and thereby prevent the export of solid material.

## Conclusions

The main objective of the present study was to describe the erosion processes in drained peatland forests, and to develop calculation methods for predicting erosion from a ditch network after its maintenance and thereby to increase understanding of erosion processes. The classic deterministic approach to erosion was used in the calculations, where a threshold value determines the detachment of particles. The erosion model was applicable for non-cohesive soils and it was designed to simulate processes in a drained area with a shallow peat layer where the ditches reach the mineral subsoil. The sediment transport in a computational node (stretch of a ditch) was calculated as an equilibrium transport, which assumes an exchange of particles between the bed, the bed load layer, and the suspended load layer to equilibrate transport.

The model was tested using field data from a forested peatland catchment, where the ditch network was maintained. The calibration period was two years after the maintenance. The model was suitable for simulating short-term (first two years) changes in the drained ditch after the maintenance. The focus was on the short term processes after the ditch network maintenance, because the most important changes in sediment load from the point of view of environmental effects occur during and shortly after ditch treatments.

The modelled spatial variability of the sediment concentration in the simulation ditch was found to be controlled by changes in the ditch bottom slope. The highest concentration was computed in the nodes, where the slope was the steepest. The most influential factor for controlling the temporal variability of concentration was the water discharge rate. The concentration of suspended solids during peak flows was several orders of magnitude higher than the lowest concentration values.

The sensitivity analysis suggested that the main factors controlling erosion and sedimentation in the model were the particle size of the material in bed and in suspension, the roughness height of the bed, the Manning coefficient, the bed slope, and the water discharge in this order of importance. Erosion and sedimentation were found to be located in the places where the flow velocity changed: soil particles were eroded where the flow accelerated and deposited where the flow slowed down. Further development of the model calls for testing against comprehensive field measurements of sediment load connected to changes in channel dimensions.

*Acknowledgements:* This work was conducted in the research project HAME (Tools for Water Protection in Forestry), which is coordinated by the Finnish Forest Research Institute (METLA) and funded by the Ministry of Agriculture and Forestry. The article was written, while the corresponding author was working in the Academy of Finland (project 121991). The data for the study was kindly provided by METLA's METVE project, the Geological Survey of Finland (GTK), and the Finnish Meteorological Institute. Thanks are due to Dr. Jukka Alm for his valuable comments on the manuscript. Dr. Samuli Joensuu from the Forestry Development Centre Tapio, Prof. Leena Finér from METLA, Jouko Saarelainen from GTK, and Dr. Teemu Kokkonen from the Helsinki University of Technology are acknowledged for their support.

## References

- Ahti E., Joensuu S. & Vuollekoski M. 1995. Laskeutusaltaiden vaikutus kunnostusojitusalueiden kiintoaineshuuhoutumaan. *Suomen ympäristö* 2: 139–155.
- Ahtiainen M. & Huttunen P. 1999. Long-term effects of forestry managements on water quality and loading in brooks. *Boreal Env. Res.* 4: 101–114.
- Bohling B. 2005. Estimating the risk for erosion of surface sediments in the Mecklenburg Bight (south-western Baltic Sea). *Baltica* 18: 3–12.
- Doten C.O. & Lettenmaier D.P. 2004. *Prediction of sediment erosion and transport with the distributed hydrology-soil-vegetation model*. University of Washington, Department of Civil and Environmental Engineering. Water Resources Series, Technical Report no. 178.
- Drebs A., Nordlund A., Karlsson P., Helminen J. & Rissanen P. 2002. *Tilastoja Suomen ilmastosta 1971–2000. Climatological statistics of Finland 1971–2000*. Finnish Meteorological Institute.
- Dun S., Wu J.Q., Elliot W.J., Robichaud P.R. & Flanagan D.C. 2006. *Adapting the Water Erosion Prediction Project (WEPP) model to forest conditions*. American Society of Agricultural and Biological Engineers. An ASABE Section Meeting Presentation, Paper no. 062150.
- Einstein H.A. 1950. *The bed-load function for sediment transportation in open channel flows*. Technical bulletin no. 1026, Department of Agriculture, Washington D.C.
- El-Sadek A., Feyen J. & Berlamont J. 2001. Comparison of models for computing drainage discharge. *J. Irrig. Drain. E.-ASCE* 127: 363–369.
- Exner F.M. 1925. Über die Wechselwirkung zwischen Wasser und Geschiebe in Flüssen. *Sitzungsberichte d. Akad. d. Wiss., math.-naturw. Klasse*, Bd. 134, Abt. IIa: 165–203.
- Finnish Statistical Yearbook of Forestry 2005. Finnish Forest Research Institute.
- Goodell C.R. 2002. Stable channel design functions. In: *HEC-RAC river analysis system*, Hydraulic Reference Manual ver. 3.1, US Army Corps of Engineers, Hydrologic Engineering Center, pp. 15–15.21.
- Graf W.H. 1984. *Hydraulics of sediment transport*. Water resources publications, BookCrafters Inc., Chelsea, Michigan, USA.
- Hosia L. 1980. *Pienten uomien virtausvastuserroin*. Vesihallitus, Tiedotus 199.
- Joensuu S. 1994. *Laskeutusaltaiden täytyminen ja täyttymisenopeuteen vaikuttavat tekijät metsäojitusalueilla*. Licentiate's dissertation, Department of Forest Ecology, University of Helsinki.
- Joensuu S. 1999. *Ojitetujen soiden puuntuotanto ja ympäristönhoito*. Metsätalouden kehittämisskeskus Tapio.
- Joensuu S. 2002. *Effects of ditch network maintenance and sedimentation ponds on export loads of suspended solids and nutrients from peatland forests*. Finnish Forest Research Institute, Research papers 868.
- Joensuu, S., Ahti, E. & Vuollekoski, M. 1999. The effects of peatland forest ditch maintenance on suspended solids in runoff. *Boreal Env. Res.* 4: 343–355.

- Kleinhans M.G. & van Rijn L.C. 2002. Stochastic prediction of sediment transport in sand-gravel bed rivers. *J. Hydraul. Eng.* 128: 412–425.
- Koivusalo H., Ahti E., Laurén A., Kokkonen T., Karvonen T., Nevalainen R. & Finér L. 2008. Impacts of ditch cleaning on hydrological processes in a drained peatland forest. *Hydrol. Earth Syst. Sc.* 12: 1211–1227.
- Koivusalo H., Kokkonen T., Laurén A., Ahtiainen M., Karvonen T., Mannerkoski H., Penttinen S., Seuna P., Starr M. & Finér L. 2006. Parametrisation and application of a hillslope hydrological model to assess impacts of a forest clear-cutting on runoff generation. *Environmental Modelling & Software* 21: 1323–1339.
- Laurén A., Finér L., Koivusalo H., Kokkonen T., Karvonen T., Kellomäki S., Mannerkoski H. & Ahtiainen M. 2005. Water and nitrogen processes along a typical water flowpath and streamwater exports from a forested catchment and changes after clear-cutting: a modelling study. *Hydrol. Earth Syst. Sci.* 9: 657–674.
- Liu Z. 2001. *Sediment transport*. Laboratoriet for Hydraulik og Havnebygning, Institutet for Vand, Jord og Miljøteknik, Aalborg Universitet.
- Meteorol. Yearb. Finland* 1992. Finnish Meteorol. Inst.
- Meteorol. Yearb. Finland* 1993. Finnish Meteorol. Inst.
- Meteorol. Yearb. Finland* 1994. Finnish Meteorol. Inst.
- Nash J.E. & Sutcliffe, J.V. 1970. River flow forecasting through conceptual models. Part I. A discussion of principles. *J. Hydrol.* 10: 282–290.
- Parker G., Paola C. & Leclair S. 2000. Probabilistic Exner sediment continuity equation for mixtures with no active layer. *J. Hydraul. Eng.* 126: 818–826.
- Rákóczi L. 1987. Selective erosion of noncohesive bed materials. *Physical Geography* 69: 29–35.
- Shields A. 1936. Anwendung der Aehnlichkeitsmechanik und der Turbulenzforschung auf die Geschiebebewegung. *Mitteilungen der Preussischen Versuchsanstalt für Wasserbau und Schiffbau* 26: 5–26.
- Sillanpää P., Bilaletdin Ä., Kaipainen H., Frisk T. & Sallantausta T. 2006. Metsätalouden aiheuttaman kuormituksen laskentamenetelmä. *Suomen ympäristö* 817: 1–41.
- Vanoni V.A. (ed.) 2006. *Sedimentation engineering*. ASCE Manuals and Reports on Engineering Practice no. 54.
- Van Rijn L.C. 1984a. Sediment transport, Part I: Bed load transport. *J. Hydraul. Eng.* 110: 1431–1456.
- Van Rijn L.C. 1984b. Sediment transport, Part III: Bed forms and alluvial roughness. *J. Hydraul. Eng.* 110: 1733–1754.
- Van Rijn L.C. 1987. *Mathematical modelling of morphological processes in the case of suspended sediment Transport*. Ph.D. thesis, Delft University of Technology, the Netherlands.
- Wang J., Sui J. & Karney B.W. 2008. Incipient motion of non-cohesive sediment under ice cover — an experimental study. *J. Hydrodynamics* 20: 117–124.

## Appendix

### Equations used in sediment load calculation

$$\delta_b = 0.3d_{50}D_*^{0.7}T^{0.5} \quad \text{Saltation height (m), } \max(\delta_b) = 10d_{50} \quad (\text{A1})$$

$$u_b = 1.5 \left[ (s-1)gd_{50} \right]^{0.5} T^{0.6} \quad \text{Particle velocity (m s}^{-1}\text{)} \quad (\text{A2})$$

$$c_b = 0.117 \frac{T}{D_*} \quad \text{Bed-load concentration (m}^3 \text{ m}^{-3}\text{)} \quad (\text{A3})$$

where  $d_{50}$  is the median particle diameter (m) of the bed material,  $D_*$  is the dimensionless particle parameter (see Eq. 8),  $T$  is the transport stage parameter,  $s$  is the relative density ( $\rho_s/\rho$ , where  $\rho_s$  is the soil particle density and  $\rho$  is the water density), and  $g$  is the acceleration due to gravity ( $\text{m s}^{-2}$ ). The transport stage parameter is calculated as follows:

$$T = \frac{(u'_*)^2 - (u_{*cr})^2}{(u_{*cr})^2} \quad 10^{-10} \leq T \leq 25 \quad (\text{A4})$$

$$\begin{cases} u'_* = \bar{u} \left( \frac{g^{0.5}}{C'} \right) & C' > 1 \\ u'_* = 0.00001 & C' \leq 1 \end{cases} \quad (\text{A5})$$

$$C' = 18 \log \left( \frac{12R_b}{K_s} \right) \quad (\text{A6})$$

where  $u_{*cr}$  is the critical bed-shear velocity according to Shields (1936) ( $m s^{-1}$ ), which can be calculated using Eqs. 6 and 7, is the effective bed-shear velocity related to grains ( $m s^{-1}$ ),  $C'$  is the Chézy coefficient related to grains, is the depth-averaged flow velocity ( $m s^{-1}$ ),  $K_s$  is the bed roughness height (m), and  $R_b$  is the hydraulic radius (m) related to the bed. The hydraulic radius is defined as  $R_b = A/P$ , where  $A$  is the cross-sectional area of the flow ( $m^2$ ) and  $P$  is the wetted perimeter (m).

$$c(z) = c_a \left( \frac{h-z}{z} \frac{a}{h-a} \right)^{z_r} \quad \text{Concentration (m}^3 \text{ m}^{-3}\text{) on the vertical level } z \text{ (m)} \quad (A7)$$

$$u(z) = \frac{u_*}{\kappa} \ln \left( \frac{z}{z_0} \right) \quad \text{Velocity (m s}^{-1}\text{) on the vertical level } z \text{ (m)} \quad (A8)$$

$$c_a = 0.015 \frac{d_{s0}}{a} \frac{T^{1.5}}{D_*^{0.3}} \quad \text{Reference concentration (m}^3 \text{ m}^{-3}\text{) at level } a \quad (A9)$$

where  $z_0$  is the zero-velocity level (for the assumed hydraulically rough flow  $z_0 = 0.033K_s$ ),  $h$  is the water depth and upper boundary for suspended load layer (m), and  $a$  is the lower boundary for the suspended load layer (m). The variable  $a$  is defined as

$$\begin{cases} a = 0.99h & \max(0.5\Delta, K_s) \geq 0.99h \\ a = \max(0.5\Delta, K_s) & 0.99h > \max(0.5\Delta, K_s) > a_{mn} \\ a = a_{mn} & \max(0.5\Delta, K_s) \leq a_{mn} \end{cases} \quad (A10)$$

$$a_{mn} = \max(2d_{s0}, 0.01h) \quad (A11)$$

$$\Delta = h \left[ 0.11 \left( \frac{d_{s0}}{h} \right)^{0.3} (1 - e^{-0.5T}) (25 - T) \right] \quad (A12)$$

where  $a_{mn}$  the lower limit of  $a$  (m) and  $\Delta$  is the bed-form height (m). The Rouse number is

$$Z_r = \frac{w}{\beta \kappa u_*} \quad (A13)$$

where  $\beta$  is the diffusion coefficient ( $\beta = 1$ ),  $\kappa$  is von Karman's constant ( $\kappa = 0.4$ ), and  $w$  is the settling velocity ( $m s^{-1}$ ), defined as:

$$\begin{cases} w = \frac{1}{18} \frac{(s-1)gd_s^2}{v} & d_s < 0.0001 \\ w = 10 \frac{v}{d_s} \left\{ \left[ 1 + \frac{0.01(s-1)gd_s^3}{v^2} \right]^{0.5} - 1 \right\} & 0.0001 \leq d_s \leq 0.001 \\ w = 1.1 [(s-1)gd_s]^{0.5} & d_s > 0.001 \end{cases} \quad (A14)$$